

Permeability and Micromechanical Properties of Silk Ionomer Microcapsules

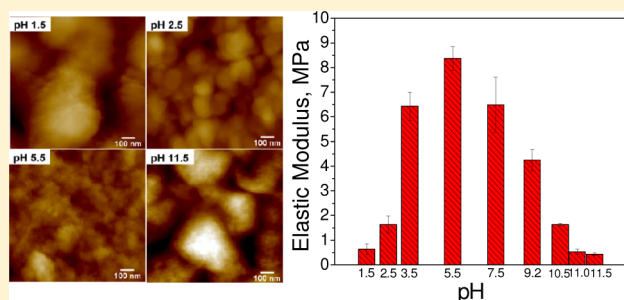
Chunhong Ye,^{†,‡} Irina Drachuk,[‡] Rossella Calabrese,[§] Hongqi Dai,[†] David L. Kaplan,[§] and Vladimir V. Tsukruk^{‡,*}

[†]School of Chemical Engineering, Nanjing Forestry University, Nanjing, Jiangsu 210037, P. R. China

[‡]School of Materials Science and Engineering, Georgia Institute of Technology, Atlanta, Georgia 30332, United States

[§]Department of Biomedical Engineering, Tufts University, 4 Colby Street, Medford, Massachusetts 02155, United States

ABSTRACT: We studied the pH-responsive behavior of layer-by-layer (LbL) microcapsules fabricated from silk fibroin chemically modified with different poly amino acid side chains: cationic (silk-poly L-lysine, SF-PL) or anionic (silk-poly-L-glutamic acid, SF-PG). We observed that stable ultrathin shell microcapsules can be assembled with a dramatic increase in swelling, thickness, and microroughness at extremely acidic (pH < 2.5) and basic (pH > 11.0) conditions without noticeable disintegration. These changes are accompanied by dramatic changes in shell permeability with a 2 orders of magnitude increase in the diffusion coefficient. Moreover, the silk ionomer shells undergo remarkable softening with a drop in Young's modulus by more than 1 order of magnitude due to the swelling, stretching, and increase in material porosity. The ability to control permeability and mechanical properties over a wide range for the silk-based microcapsules, with distinguishing stability under harsh environmental conditions, provides an important system for controlled loading and release and applications in bioengineering.



INTRODUCTION

Encapsulation and delivery of active ingredients such as drugs, proteins, flavors or living cells is becoming increasingly important for a wide variety of applications and technologies in the food industry, for drug delivery, and in biology and biomedicine.^{1–13} Intensive research has been directed to address the specific requirements of encapsulation: interfacial emulsion polymerization,¹⁴ coacervation or gelation of polymer,¹⁵ fluid extrusion,¹⁶ lipid-based liposomes¹⁷ and assembly of polymer.¹⁸ A versatile method for encapsulation should provide easily controlled size, permeability, mechanical strength, compatibility, and high yield.^{19,20} Tunable size of encapsulated media allows flexibility in applications and choices of encapsulation routines; controlled permeability enables loading and unloading behavior to be modulated, selective encapsulation of macromolecules, and timed release; adjustable mechanical properties can protect entrapped material to withstand varying mechanical loads in different environments or enable release by defined shear forces. Finally, biocompatibility of encapsulating media is important for biological and biomedical applications, such as for cells encapsulation, drug delivery, and tissue engineering and regeneration.^{21–25}

Polyelectrolyte multilayer assemblies fabricated by layer-by-layer (LbL) assembly of different complementary components onto the surface of colloid particles, followed by core dissolution, provides a simple and widely adaptable route for encapsulation and release.^{26–28} A variety of intermolecular interactions such as ionic pairing,²⁹ hydrogen bonding,³⁰

covalent bonding³¹ and specific recognition³² can be used as the driving force for the assembly, which enables the use of a wide range of polymers and nanoparticles in the construction of the LbL shell. The microcapsule size can be varied from a few tens of nanometers to hundreds of micrometers, and the shape can be spherical, tetrahedral or cubic by employing various templates.³³ Furthermore, depending on the nature of the polymer utilized, LbL assemblies can exhibit multiresponsive behaviors when exposed to different external stimulations, such as pH, temperature, light, and ionic strength, which enables the manipulation of permeability, morphology and mechanical properties.^{34–41} However, the cytotoxicity of synthetic polymer LbL shells caused by the use of cationic polyelectrolytes is a main limitation for application of these systems in the field of biology.⁴² Microcapsules, with robust shells and stability under harsh environments, such as extreme acidic and basic conditions, high shear force, and biofluids, are rare.

Silk fibroin is a natural protein from silkworms and spiders and has been widely utilized in biomaterial composites.^{43,44} The versatility of silk is attributed to the outstanding mechanical properties (a unique combination of high elastic modulus, elongation to break and toughness),⁴⁵ near-perfect transparency in the visible range⁴⁶ and biological properties (biocompatibility and tunable biodegradability), which make

Received: June 15, 2012

Revised: July 23, 2012

Published: July 26, 2012

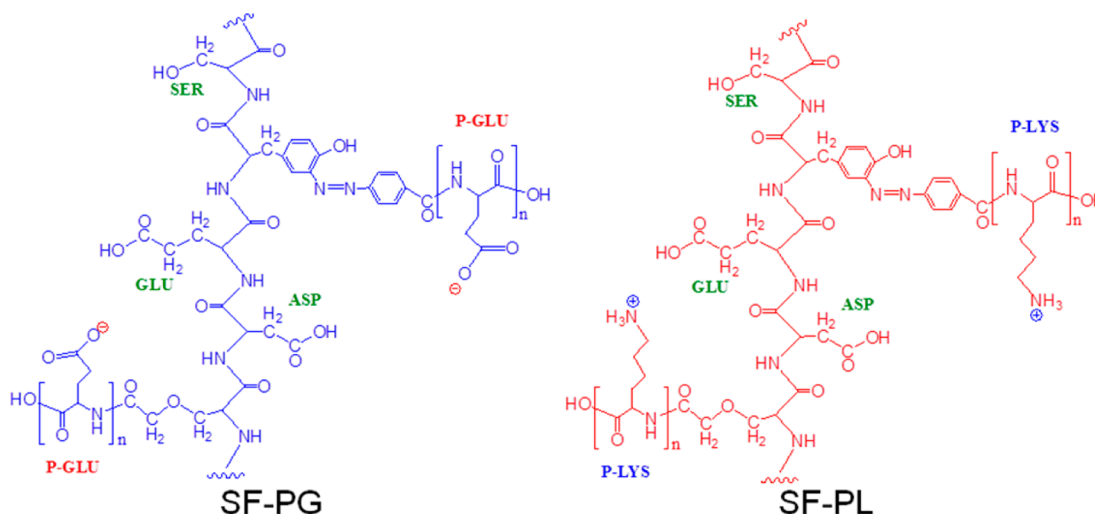


Figure 1. Chemical structure of silk-poly(amino acid) ionomers: silk-poly-L-glutamic acid (SF-PG) and silk-poly-L-lysine (SF-PL).

silk-based materials excellent candidates for drug delivery systems, scaffolds for tissue and biosensor engineering. However, building microconstructions from proteins is challenging because of their poor stability. Up to now, final silk structures (ultrathin films and microcapsules) have been stabilized by the formation of β -sheets.^{47–49} However, our recent study described a different strategy, based on ion pairing of the poly amino acid functionalized silk ionomers.⁵⁰ By utilizing these natural components, stable and robust silk-based LbL microcapsules were successfully fabricated with highly reversible pH responsive features and controlled encapsulation and release abilities.⁵¹

In the present study, we focus on quantitative analysis of the critical physical (transport and mechanical) properties of the silk ionomer microcapsules fabricated by combining ionic pairing and covalent cross-linking as has been very recently introduced.⁵¹ Both shell permeability and stiffness along with shell morphology have been measured for different fabrication and environmental conditions. These microcapsules demonstrated pH-induced permeability at extreme acidic ($\text{pH} < 2.5$) and basic ($\text{pH} > 11.0$) conditions with 2 orders of magnitude increases in the diffusion coefficient, accompanied by dramatic changes in morphology but without compromising capsule integrity. Furthermore, the silk LbL shell exhibited a higher elastic modulus than traditional hydrogen-bonded microcapsules composed of synthetic polyelectrolytes, and the stiffness is widely tunable by external pH conditions and additional covalent cross-linking. These silk-based microcapsules with adjustable permeability and outstanding mechanical properties may serve as a new promising platform for bioengineering applications.

EXPERIMENTAL SECTION

Materials. Silk-poly(amino acid)-based ionomers were obtained using our previously published method (Figure 1).⁵⁰ First, the silk fibroin was extracted from *Bombyx mori* cocoons according to our established procedures.⁵² The tyrosine and serine residues of the SF backbone were chemically modified via diazonium coupling and chloroacetic acid reaction, respectively, leading to a silk derivative enriched in carboxyl groups; subsequently, one of the silk-poly(amino acid)-based ionomers (SF-PG) was obtained by grafting poly-L-glutamic acid onto silk fibroin (SF) to achieve a high carboxyl content. In contrast, SF-PL represents silk fibroin modified with poly-L-lysine side groups to enrich amine group content.

Silica spheres with a diameter of $4.0 \pm 0.2 \mu\text{m}$ as 10% dispersions in water were obtained from Polysciences, Inc. Sodium phosphate dibasic, sodium phosphate monobasic, and hydrofluoric acid (HF 48–51%) were purchased from BDH. Ammonium fluoride (AF) was obtained from Alfa Aesar. Branched polyethylenimine (PEI) with $M_n = 10\,000$, fluorescent isothiocyanate (FITC), and FITC-dextrans with different molecular weights were obtained from Sigma-Aldrich. The cross-linker, 1-ethyl-3-[3-dimethylaminopropyl] carbodiimide hydrochloride (EDC), was obtained from TCI. All materials were used without further purification. The water used in all experiments was Barnstead Nanopure water with a resistivity above $18.2 \text{ M}\Omega \text{ cm}$. Single-side polished silicon wafers of {100} orientation (University Wafer Co) were cut to a typical size of $10 \text{ mm} \times 20 \text{ mm}$ and cleaned in a piranha solution as described elsewhere.⁵³

Fabrication of “PEI-(SF-PG/SF-PL)_n” Capsules. Silica spheres were dispersed in 0.5 mg/mL PEI solution (prepared in 0.1 M NaCl, pH 7) to make a prime layer to stabilize the LbL process. Then silica spheres were dispersed in 1 mg/mL silk fibroin-poly-L-glutamic acid, SF-PG, prepared in 0.05 M phosphate buffer at pH 5.5, followed by SF-PL deposition as redispersion in 1 mg/mL silk fibroin-poly-L-lysine solution, SF-PL, prepared in 0.05 M phosphate buffer at pH 5.5. Multilayer capsules were obtained by repeating the alternating deposition of SF-PG and SF-PL components (Figure 2). Each

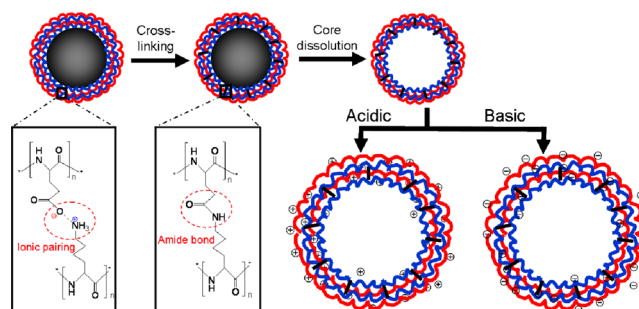


Figure 2. LbL self-assembly of silk-poly(amino acid) ionomer microcapsules through ionic pairing followed by covalent cross-linking.

deposition was carried out with slow rotation to avoid the formation of air bubbles for 15 min, followed by two wash cycles in phosphate buffer with pH 5.5 by centrifugation at 1000 rpm for 1 min to remove the excess of polyelectrolytes.

All capsules were cross-linked with 1-ethyl-3-[3-dimethylaminopropyl] carbodiimide hydrochloride (EDC) according to the established procedures.⁵⁴ The silica spheres with PEI(SF-PG/SF-PL)_n multilayers were added to 5 mg/mL EDC solution (prepared in 0.05 M phosphate

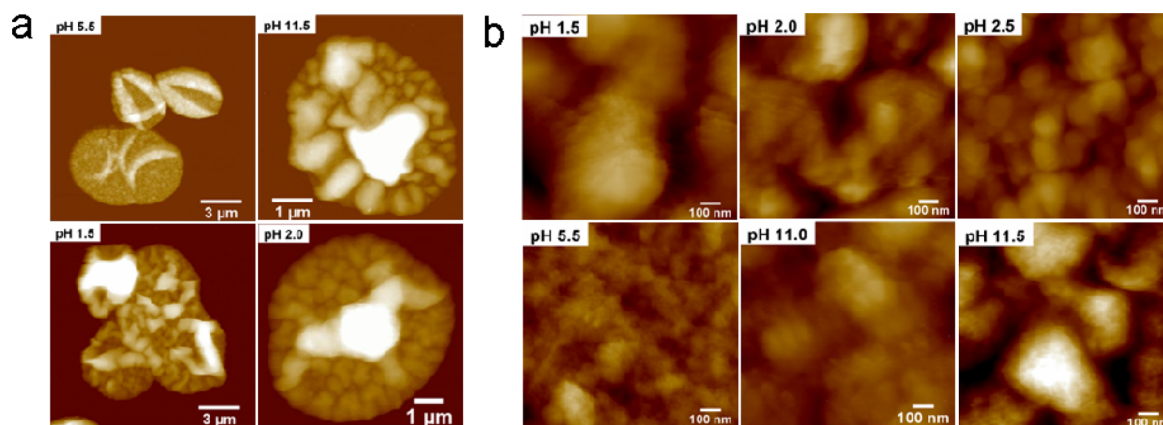


Figure 3. Morphology of silk ionomer microcapsule at different pHs in liquid state. (a) AFM topography images of swollen PEI-(SF-PG/SF-PL)₅ capsules in pH 5.5 and 11.5 (Z-scale: 1,000 nm) and pH 1.5 and 2.0 (Z-scale: 2,000 nm) phosphate buffer solutions. (b) High resolution AFM height images of swollen PEI-(SF-PG/SF-PL)₅ capsules in pH 1.5, 2.0, 2.5, 5.5, 11.0, and 11.5 phosphate buffer solutions (Z-scale: 200 nm).

buffer at pH 5.5) for 40 min and then washed with phosphate buffer at pH 5.5 to remove excess coupling agent. To dissolve the silica cores, the particles were exposed to 1 M HF/4 M NH₄F solution (pH ~5.5) overnight, followed by dialysis with slide-A-lyzer dialysis cassettes (100 000 MWCO, Thermal Scientific) against Nanopure water at pH 5.5 for 72 h with repeated changes of water (Figure 2).^{55,56}

CHARACTERIZATION

Atomic Force Microscopy (AFM). Surface topography of the hollow capsules in dried and swollen states was examined by AFM.⁵⁷ The height and phase images were collected with a Dimension-3000 AFM (Digital Instruments) in tapping mode using silicon V-shape cantilevers having spring constants of 46 N/m for imaging in air. For the morphology of the swollen state at different pHs, a scanAsyst-fluid mode on a Dimension-Icon (Veeco) was employed using a liquid cell and a tip with a spring constant of 0.7 N/m. Samples were prepared by placing a droplet of hollow capsule suspension on a precleaned silicon wafer and drying in air prior to AFM scanning. During the scanning in liquid, phosphate buffer solution with different pHs was added to the predried capsules. The capsule single wall thickness was determined as half of the height of the collapsed flat regions on dried and swollen capsules using bearing analysis from NanoScope software to generate height histograms. The microroughness was measured in smooth microcapsule regions from selected 1 μm × 1 μm areas without wrinkles.^{58,59}

Micromechanical properties of silk ionomer capsules were measured by force-volume mode on the Dimension-3000 microscope in both dry and swollen states. Force–distance curves were collected by micromapping with 16 × 16 point arrays over a 1 μm × 1 μm area selected without wrinkles. Silicon nitride tips with spring constants of 6.0 and 0.7 N/m were used in dry and liquid state, respectively. The spring constants of the cantilevers were determined by thermal tuning. The tip radius was estimated by scanning a reference standard sample with 5 nm gold nanoparticles. Mechanical measurements of capsules in the swollen state were performed with a liquid cell in phosphate buffer adjusted to specified pH values.

The collected data were processed with a custom-made micromechanical analysis (MMA) software according to the well-established procedure.^{59–61} A parabolic Snedoon's model was utilized to calculate Young's modulus by processing the force–distance curves collected in the elastic regime at the

selected flat surfaces without wrinkles from at least three individual capsules to ensure representative results.

Confocal Laser Scanning Microscopy (CLSM). Confocal images of capsules were obtained with LSM 510 vis confocal microscope equipped with 63 × 1.4 oil immersion objective lens (Zeiss). Capsules were visualized by adding FITC solution (1 mg/mL in phosphate buffer at pH 5.5) to the capsule suspension in Lab-Tek chambers (Electron Microscopy Science). Excitation/emission wavelengths were 488/515 nm. To investigate capsule permeability, fluorescent recovery after photobleaching (FRAP) was investigated by photobleaching FITC-dextran fluorescent molecules inside the microcapsule with CLSM.⁶²

A drop of hollow capsule suspension was added to a Lab-Tek chamber, mixed with 200 μm of 1 mg/mL FITC-labeled dextran solution with different molecular weights (prepared in phosphate buffer at different pHs) and allowed to settle for several hours to make sure the fluorescent intensities inside and outside of the capsule were same. Then a laser beam (488 nm) was focused within a region inside a capsule and pulsed at 100% intensity to photobleach the dye molecules. Each FRAP started with 5 prebleached scans, followed by 25–30 iterations of bleaching to make sure the fluorescent intensity inside the capsule was reduced by 40–60% while avoiding damage to the capsule. The fluorescence recovery was monitored by capturing scans of 3 ms exposure at low laser intensity (3% of maximum). The recovery was considered complete when the fluorescence of the photobleached region leveled off. The FRAP recovery curves were analyzed using an established procedure.^{62,63} The recovery curve of the fluorescence intensity, I , as a function of time, t , was fit by a function

$$I = I_0(1 - e^{-At}) \quad (1)$$

where I_0 represents the initial fluorescence intensity. The coefficient A is related to the diffusion coefficient, D , according to equation:

$$A = 3P/r = 3D/rh \quad (2)$$

Which is valid for diffusion through a spherical wall with radius r and thickness h .

RESULTS AND DISCUSSION

Silk Shell Morphologies. Silk-polyamino acid ionomers, obtained by selective modification side groups of silk protein

backbone to enrich either cationic (silk-poly-L-lysine, SF-PL) or anionic (silk-poly-L-glutamic acid, SF-PG) charges, were utilized to prepare hollow microcapsules by LbL assembly (Figure 1).

The capsules were stable over a wide pH range, 1.5 to 12.0, and showed a remarkable degree of reversible swelling/deswelling when exposed to pH conditions below 2.0 and above 11.0 (Figure 2). As has been demonstrated in our previous publication, the diameter of silk ionomer microcapsule increased for $3.8 \pm 0.2 \mu\text{m}$ at pH 5.5 to $5.3 \pm 0.2 \mu\text{m}$ at pH 1.5 and $5.7 \pm 0.2 \mu\text{m}$ at pH 12.⁵¹

In order to understand the pH responsive properties of the silk ionomer microcapsules, the morphology of the capsules was monitored upon exposure to different pH conditions (Figure 3a). Upon drying the hollow silk microcapsules on a solid substrate, random wrinkles are formed due to shell collapse.^{64,65} Even by exposing the predried capsules to the aqueous solutions, the capsules still kept the wrinkled morphology. However, upon exposure to the solution with a pH above 10.5 and below 3.5 (adjusted by 0.05 M phosphate buffer), the topography significantly changed. The silk LbL shell swelled for capsules at pH 2.0 when compared to the same bilayer number capsules at pH 5.5. Further reducing the solution pH to 1.5 resulted in uneven and ruffled morphologies observed from AFM. The same phenomenon was obtained at pH above 11.5.

The dramatic change of grainy texture of shells was also revealed by high resolution AFM images at different pHs (Figure 3b). The surface morphology of silk materials undergoing partial transformation of secondary structure associates with the grainy topography at pH 5.5.⁶⁶ The grainy structure gradually formed as the capsules were exposed to pH 2.5, 2.0, and 1.5, respectively. The same change happened upon exposure to basic conditions.

The thickness of silk ionomer microcapsules with 5 bilayers was measured by AFM cross sections in the swollen state at pHs from 1.5 to 11.5 (Figure 4a). The shell thickness increased gradually from $87 \pm 6 \text{ nm}$ (pH 5.5) to $107 \pm 6 \text{ nm}$ (pH 3.5) and $103 \pm 8 \text{ nm}$ (pH 11.0) and then followed by dramatic swelling to $204 \pm 15 \text{ nm}$ for pH below 2.0. The capsules showed a nonuniform swelling at pH 11.5, where some regions had high swelling and a reached thickness of $201 \pm 35 \text{ nm}$, whereas some regions remained at about the same thickness as at pH 5.5. The values of thickness even in neutral conditions were significantly higher than typical values for hydrogen bonded capsules within the range from 20 to 35 nm associated with the different components and molecule weights.^{67,68}

The same trend was observed for changes in shell microroughness, as measured in selected smooth (without wrinkles) areas of $1 \times 1 \mu\text{m}^2$. The capsules exhibited an almost constant roughness (13.5–16.5 nm) over a wide pH range from 3.5 to 10.5, much higher than usually observed for electrostatic based LbL films (around 1–2 nm)⁶⁹ but common for diffusion-enhanced LbL assembly with aggregated and porous morphologies.⁷⁰ These features were close in terms of roughness to those previously reported for hydrogen bonded microcapsules employing a PEI-prelayer (in the range of 13–15 nm).⁶⁷

Furthermore, the microroughness dramatically increased for pH values below 3.5 and above 10.5, and reached a value of $27.5 \pm 1 \text{ nm}$ at (pH 1.5) and $37.5 \pm 3 \text{ nm}$ (pH 11.5) (Figure 4). Such a remarkable increase in surface microroughness is consistent with the steady development of domain morphol-

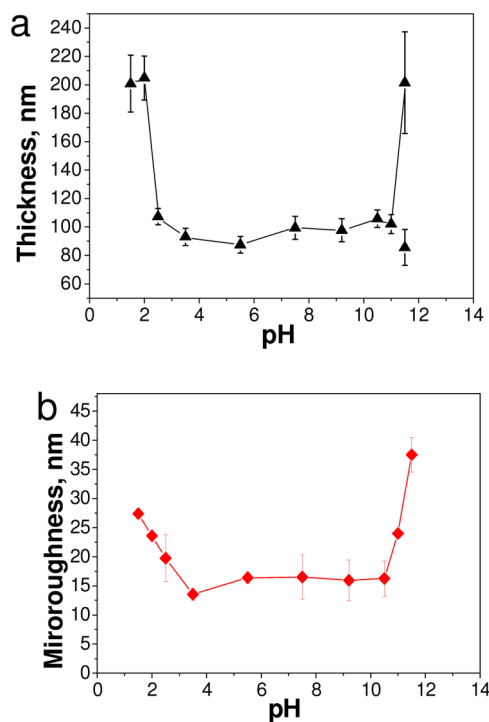


Figure 4. pH induced variation of silk ionomer microcapsules physical features. (a) pH-triggered swelling of PEI-(SF-PG/SF-PL)₅ hollow capsules in pH range from 1.5 to 11.5. (b) Microroughness of PEI-(SF-PG/SF-PL)₅ hollow capsules as a function of pH.

ogies with the dimensions enlarged from 30–40 nm to about 300 and 400 nm for pH 11.5 and 1.5, respectively. The grainy structure is a common phenomenon for silk materials,^{48,71} due to local aggregation, and the responsive changes of domain sizes are attributed to reduced ionic pair bonding upon exposure to extremely basic and acid pHs.

The distinct pH-dependent changes in morphology of silk ionomer capsules can be related to a reduction of ionic bonding in the LbL thin shell at extreme conditions. As known, polyglutamic acid and polylysine utilized here for preparing the pairing of silk ionomers have $pK_a \sim 3.5$ and ~ 9 , respectively.⁷² The negative charge of SF-PG gradually decreased due to the protonation of carboxyl group below its pK_a . There is a higher degree of deprotonation of amino groups on SF-PL and a lower positive charge on the SF-PL when the pH is above its pK_a . The result is consistent with the variation of zeta-potential of hollow capsules in the pH range from 1.5 to 12.0 which was described in our previous publication, where the zeta-potential was negative in the pH range from 3.5 to 7.5 and then increased to positive values for pHs below 2.5 and more negative above pH 7.5.⁵¹

Only capsules with additional EDC-induced cross-linking with amide bonds between carboxylic groups on SF-PG and primary amine groups on SF-PL exhibited uniform swollen shapes under extremely acidic and basic conditions indicating light permanent cross-linking (Figure 2). Indeed, the untreated microcapsules are totally dissolved when exposed to acidic (pH < 1.5) or basic environments (pH > 11.5). The FTIR spectra for microcapsules with and without cross-linking did not indicate significant detectable changes thus confirming very low degree of cross-linking. In fact, the silk backbone is composed of repeated amino acid units through amide bonds,⁷³ which resulted in a strong carbonyl peak of amide bonds for silk-based

Table 1. Thickness and Microroughness of PEI-(SF-PG/SF-PL)₅ Microcapsules with Different Cross-Linking Times in the Dry and Swollen States (pH 6.0)

cross-linked time, min	thickness, nm			microroughness, nm		diameter, μm
	dry	swollen	swelling %	dry	swollen	swollen
0	48.0 \pm 2.1	86.4 \pm 1.9	80.0	8.7 \pm 1.3	12.7 \pm 2.3	3.74 \pm 0.06
40	46.2 \pm 1.6	74.6 \pm 3.2	61.5	11.5 \pm 3.3	13.6 \pm 3.1	3.73 \pm 0.06
80	46.7 \pm 2.2	78.8 \pm 3.0	68.7	11.3 \pm 0.3	17.3 \pm 2.7	3.80 \pm 0.05
160	44.5 \pm 2.4	70.8 \pm 3.0	59.1	11.3 \pm 1.7	11.1 \pm 1.2	3.75 \pm 0.06

capsules even without cross-linking thus masking possible changes during cross-linking (Figure 2).^{54,68,74}

Significant variation of thickness and microroughness for PEI-(SF-PG/SF-PL)_n capsules was observed with different cross-linked time in dry and swollen states (Table 1). The degree of swelling decreased with increasing cross-linking time due to the higher degree of cross-linking. In addition, thickness also decreased from 48.0 \pm 2.1 to 44.5 \pm 2.2 nm indicating densification of the shells upon cross-linking. Comparing overnight cross-linking from the literature,^{54,75} the cross-linking time was set to 40 min to obtain stable capsules at extremely acidic and basic pHs while minimizing the effect of cross-linking on capsule properties and avoid excessive stiffening. A grainy surface texture and with significant variation in microroughness at different pHs of the silk ionomer shells suggests a porous morphology to facilitate tunable permeability.⁷⁶

Silk Shell Permeability. FRAP analysis of permeability was conducted by using fluorescein isothiocyanate (FITC)-labeled dextran as a fluorescent probe with confocal microscopy (Figure 5).^{62,77,78} Focusing the laser beam onto the capsule interior and increasing the excitation intensity at 100% of maximum resulted in efficient bleaching (Figure 5a, middle). Immediately after bleaching stage and reduction of the laser power by a factor of 30, the intensity of the capsule interior gradually increased over time due to the diffusion of unbleached FITC-dextran surrounding the capsule into the interior until the intensity inside of the capsule became constant (Figure 5a, right). For quantitative analysis, the fluorescence intensity inside the bleached capsule was integrated to give intensity values for each time point, which constituted the FRAP recovery curves which can be fit with eq 1 (Figure 5b,c).

Although the number of bilayers significantly affected the cutoff molecular weight for permeation,^{48,51} the slope of the recovery curve for silk ionomer microcapsules with five bilayers was only slightly higher than that of seven and nine bilayer shells exposed to 4 kDa FITC-dextran at pH 5.5 (Figure 5b). However, much faster recovery was observed at extremely basic (pH 11.5) and acidic (pH 2.0) conditions compared to the same capsule (5 bilayers) exposed to the same molecular weight FITC-dextran (20 kDa) at pH 5.5 (Figure 5c). This finding indicates that the diffusion rate across shells is changed dramatically by pH variations.

The fluorescent intensity recovery curve fitted with theoretical permeation kinetics equations can provide permeability coefficients, which can be converted into diffusion coefficients (D) according to eq 2 with use of shell radius and thickness (Figure 6).⁷⁹ The silk ionomer capsule indicated an exponential build-up thickness with increasing bilayer number, which resulted in a significantly thicker shell of nine bilayer capsules. However, the diffusion coefficients calculated from FRAP experiments increased from 7.2 $\times 10^{-11}$ to 2.3 $\times 10^{-10}$ cm²/s with an increasing number of bilayers (for 4 kDa FITC-

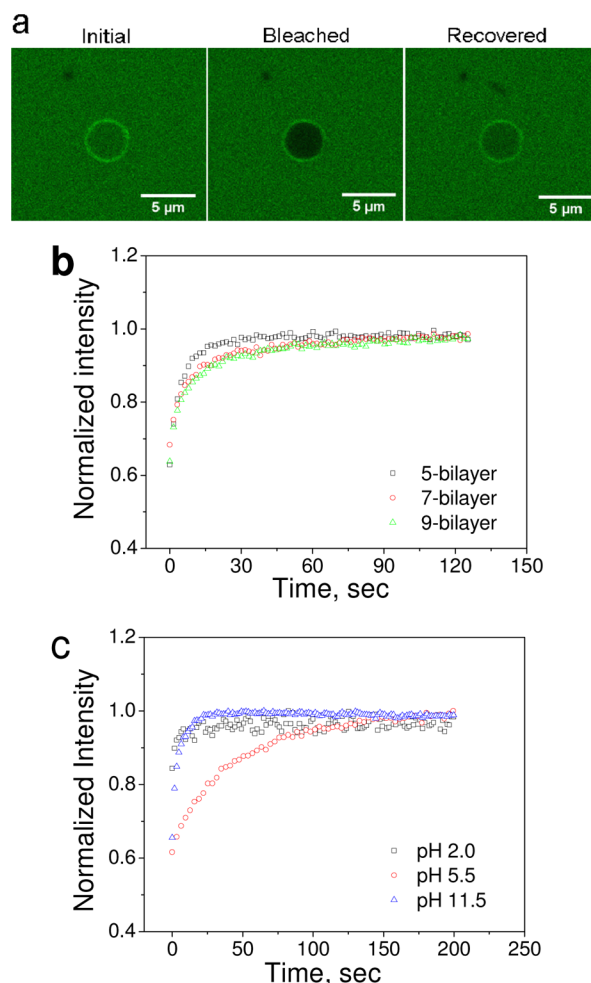


Figure 5. (a) Confocal images of PEI-(SF-PG/SF-PL)₅ capsule exposed to 4 kDa FITC-dextran solution at pH 5.5 during different stages of FRAP. (b) FRAP recovery curves of capsules with different numbers of bilayers for 4 kDa dextran at pH 5.5. (c) PEI-(SF-PG/SF-PL)₅ capsule FRAP recovering curves for 20 kDa dextran at different pHs.

dextran as a probe) at pH 5.5 indicating the role of porosity (Figure 6B). These values are much higher than those obtained for conventional low porosity ionic PAH/PSS shells where diffusion coefficients were as low as 2.7 $\times 10^{-12}$ cm²/s for low molecular weight dyes for comparable number of bilayers.⁷⁷

On the other hand, the value of the diffusion coefficient was the same order of magnitude as that reported for weakly hydrogen-bonded LbL shells with high porosity.^{65,80} We suggest that the modified silk macromolecular structure, with a hydrophobic backbone and hydrophilic pendant groups, with abundant site for hydrogen bonding contributed to a loose, porous morphology for the silk ionomer shells, resulting in the

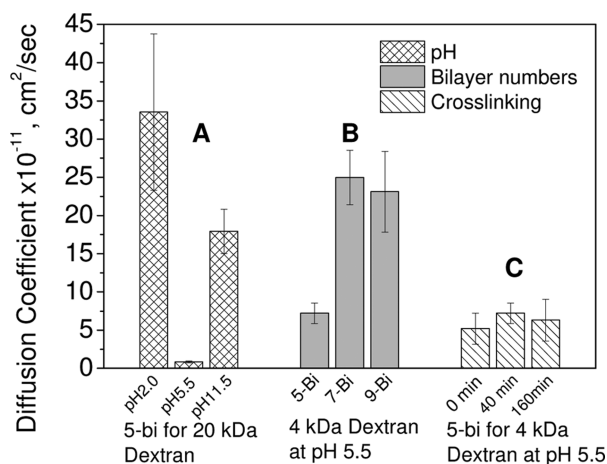


Figure 6. Diffusion coefficients of silk ionomer microcapsules. (A) pH-induced diffusion coefficient variation of PEI-(SF-PG/SF-PL)₅ hollow capsules for 20 kDa FITC-dextran. (B) Diffusion coefficient of PEI-(SF-PG/SF-PL)_n capsules with different bilayer numbers to 4 kDa FITC-dextran at pH 5.5. (C) Diffusion coefficient of PEI-(SF-PG/SF-PL)₅ capsules with different cross-linking time for 4 kDa dextran at pH 5.5.

high permeability much close to weakly bonded LbL shells than traditional ionic-based shells.

As expected, a lower diffusion coefficient was found with increasing labeled dextran molecular weight from 4 to 20 kDa (Figure 6A,B); however, when the same capsules were exposed to the dextran with the same molecular weight (20 kDa) at pH 2.0 and 11.5, the diffusion coefficients dramatically increased from 8.5×10^{-12} to 3.4×10^{-10} and 1.8×10^{-10} cm²/s, respectively (Figure 6A). Such an increase by 2 orders of magnitude indicates a more porous polymer network associated with the shell swelling and stretching at extremely acidic and basic conditions. Furthermore, the variation of cross-linking time had little effect on the diffusion behavior (Figure 6C).

Mechanical Properties of Silk Shells. Typical force–distance curves, obtained by averaging over multiple points, exhibited dramatically different shapes near the physical contact point and remarkable changes of slope in the repulsive contact regime for probing silk capsules in the dry and swollen states (Figure 7). In air, a “jump-in to contact” point was presented on the approaching curve due to the long-range attractive forces between the tip and sample, followed by an increased repulsive segment, and a high degree of hysteresis on the retracting curve. As known, strong jump-in and pull-off forces are caused by the tip–sample adhesion and capillary interactions caused by a few nm-thick layer of water on the capsule surface at ambient conditions.⁸¹ In liquid, the force–distance curves revealed lower adhesion due to the diminished capillary forces (Figure 7b) and a less sharp contact point as compared to the curve collected in air, indicating a soft repulsive surface for the swollen silk shell.

The loading curves were derived from the force–distance data by analyzing the repulsive section of the approaching curve with different deformation behavior for the silk shell in different environments (Figure 8).⁵⁹ The penetration observed from the loading curves is well-defined and less than 10% of the thickness for both dried and swollen capsules, which excludes the influence of the stiff silicon substrate.^{82,83} The linear behavior of the loading curves in Hertzian coordinates for all swollen shells reflects purely elastic deformation under the

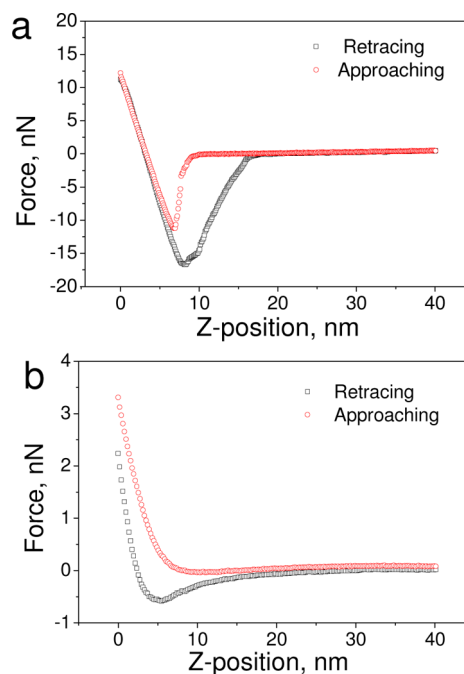


Figure 7. Force–distance curves for dried (a) and swollen (b) PEI-(SF-PG/SF-PL)₅ hollow microcapsules in air and liquid state in an approaching–retracting cycle.

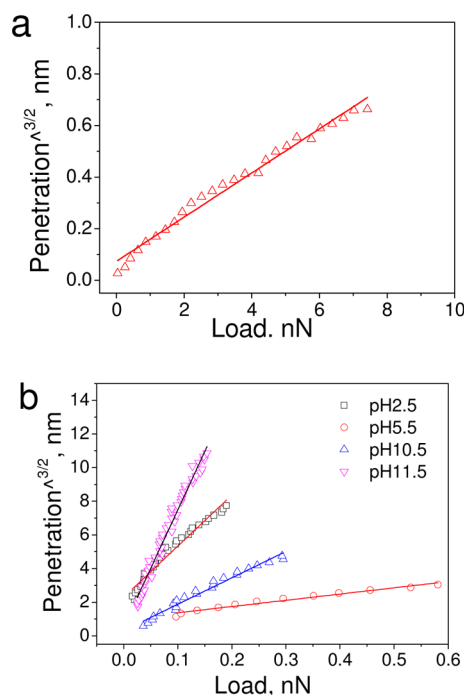


Figure 8. Loading curves in the Hertzian approximation: (a) PEI-(SF-PG/SF-PL)₅ shells in air and (b) swollen PEI-(SF-PG/SF-PL)₅ shells at different pH values.

loading force.^{84–86} The loading curve for PEI-(SF-PG/SF-PL)₅ in the liquid state demonstrated higher penetration when compared to the dry state even with very light normal loads which revealed the softening of swollen silk shells. Furthermore, the varied slope of loading curve obtained at different pH values which is directly related to their stiffness, indicates a pH-dependent elastic properties (Figure 8b). Penetration increased by a factor of 5 and 4 as the capsules were exposed to pH 2.5

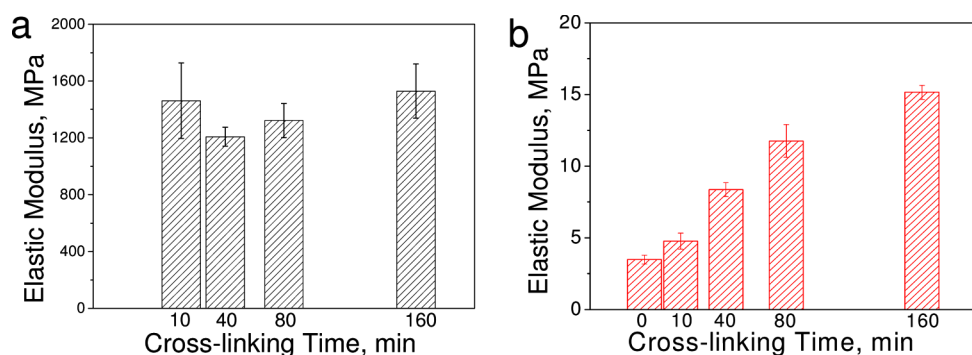


Figure 9. Young's modulus of PEI-(SF-PG/SF-PL)₃ shells in the dried state (a) and Young's modulus for swollen PEI-(SF-PG/SF-PL)₅ shells (b) for different cross-linking times.

and 11.5, respectively, indicating more compliant structures in extremely acidic and basic conditions.

The Young's modulus of the LbL silk ionomer shells with different cross-linking was determined from force spectroscopy data to vary from 1.1 to 1.8 GPa in the dry state (Figure 9a). This is the typical range for regular polyelectrolyte LbL film as well as common flexible polymers below glass transition (usually, from 1 to 5 GPa).^{87–89} On the other hand, this value is much higher than that measured for hydrogen-bond LbL capsules (600 ± 100 MPa) previously reported by our group for hydrogen-bonded shells⁶⁷ that can be attributed to the presence of stronger ionic pairing bonding, the covalent bonds formed due to EDC cross-linking, and the stiffer silk macromolecule backbone.⁴⁴

As exposed to liquid, the stiffness of the swollen capsules was significantly reduced by more than 2 orders of magnitude, to the range of around 10 MPa, due to significant swelling of the silk material in liquid, a common trend for highly compliant swollen materials with a high content of liquid.⁹⁰ The Young's modulus obtained here for silk ionomer shells is comparable but higher than that of earlier reported hydrogen-bonded capsules with elastic modulus around 4 MPa,^{68,80} which can be attributed to the covalent cross-linking and ordered domain organization of silk backbones. Moreover, gradually increased stiffness of capsules with increasing cross-linking was observed when exposed to liquid, and a dramatic reduction of modulus was observed due to swelling (Figure 9b). Indeed, the elastic modulus for shells without cross-linking was 3.5 ± 0.3 MPa, but the value increased to 15 ± 0.5 MPa for the highest cross-linking time (160 min). 5-fold increase in shell stiffness can be attributed to the increased amount of amide bonds with increased cross-linking time. The same trend was observed in earlier studies where a stiffer polyelectrolyte multilayer film for poly(L-lysine)/hyaluronan, poly(allylamine hydrochloride)/poly(L-glutamic acid) and chitosan/hyaluronan were formed by increasing cross-linking density.⁷⁵

pH-Responsive Mechanical Properties of Silk Nano-shells. The selected PEI-(SF-PG/SF-PL)₅ capsules cross-linked for 40 min were subject to various pH conditions to test their mechanical properties (Figure 10). The Young's modulus was measured within the range of 6.5 to 8.5 MPa as pH was varied from 3.5 to 7.5. Beyond this range, the shell stiffness dramatically decreased.⁷² The elastic modulus reduced by more than a factor of 10 to around 0.6 MPa at pH 1.5 which is below the pK_a of the carboxyl-terminal groups on SF-PG. Similar reduction was observed by increasing the pH above 9.2, resulting in a modulus ~0.4 MPa at pH 11.5 (Figure 10).

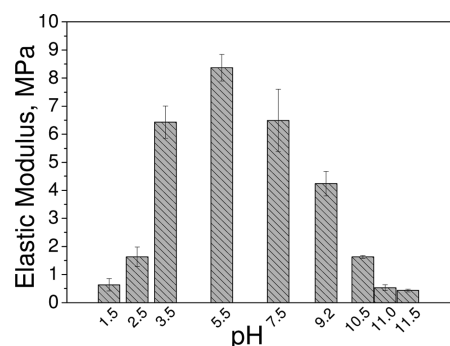


Figure 10. pH-induced variation of Young's modulus for swollen PEI-(SF-PG/SF-PL)₅ shells with cross-linking time of 40 min.

The significant decreased stiffness of the cross-linked LbL assembly of silk ionomers is associated with the remarkable swelling under extremely acidic and basic conditions. The reduction of ionic pairing between SF-PG and SF-PL for pHs below 2.5 and above 9, because the protonation of carboxyl-terminal group on SF-PG below its pK_a and deprotonation of amino groups on the SF-PL above the pK_a, reduced confinement of the silk backbones and resulted in the excessive swelling of the shells and loosened organization. The loosened polymer networks facilitated higher swelling and permeability at acidic and basic pHs, indicating more porous structures. Correspondingly, the Young's modulus decreased significantly under these conditions, because of lower density of physical cross-links, high content of water in the significantly swollen shell, and a higher porosity.⁹¹

CONCLUSIONS

In conclusion, pH-dependent mechanical properties, permeability and morphology of silk ionomer microcapsules were studied and dramatic changes in physical properties were demonstrated. The most dramatic changes were observed at extreme pH conditions around 1.5 and around 11.5. In summary, the LbL silk shell thickness swelled up to 3-fold, overall dimensions increased by a factor of 2, the diffusion coefficient increased by 2 orders of magnitude, and stiffness dropped by 1 order of magnitude at pH below 2.5 and above 11.0. These changes can be related to both the protonation of carboxyl-terminal group on SF-PG below its pK_a and deprotonation of amino groups on the SF-PL above the pK_a, reduced confinement of the silk backbones and resulted in the excessive swelling of the shells, and loosened secondary structure of silk material. It is worth noting that the silk

ionomer microcapsules with lightly cross-linked shells were extremely stable under extreme basic and acidic conditions in contrast to traditional LbL shells. Such bioderived and stable microcapsules exhibited a promise for manipulating loading–unloading behavior, cell surface engineering, and the design of biosensor systems.

AUTHOR INFORMATION

Corresponding Author

*E-mail: Vladimir@mse.gatech.edu.

Notes

The authors declare no competing financial interest.

ACKNOWLEDGMENTS

This work is supported by the Air Force Office of Scientific Research FA9550-08-1-0446, FA9550-09-1-0162, FA9550-10-1-0172, and FA9550-11-1-0233 grants (LbL fabrication of microcapsules), U.S. Department of Energy, Office of Basic Energy Sciences Award No. DE-FG02-09ER46604 (permeability and mechanics of microcapsules), the NIH AR005593 and EB002520 (synthesis of silk materials). China Scholarship Council 2010832447, Nanjing Forestry University Graduate Student Innovation Program 2011YB012 supported C.Y. The authors thank Kyle D. Anderson, Milana O. Lisunova, Olga Shchepelina, Zachary A. Combs, and Kodyath Rajesh for assistance and helpful discussion.

REFERENCES

- (1) Bédard, M. F.; Geest, B. G.; Skirtach, A. G.; Möhwald, H.; Sukhorukov, G. B. Polymeric microcapsules with light responsive properties for encapsulation and release. *Adv. Colloid Interface Sci.* **2010**, *158*, 2–14.
- (2) Bartkowiak, A.; Hunkeler, D. Alginate-oligochitosan microcapsules. II. Control of mechanical resistance and permeability of the membrane. *Chem. Mater.* **2000**, *12*, 206–212.
- (3) Chaikof, E. L. Engineering and material considerations in islet cell transplantation. *Annu. Rev. Biomed. Eng.* **1999**, *1*, 103–127.
- (4) Gibbs, B. F.; Kermasha, S.; Alli, I.; Mulligan, C. N. Encapsulation in the food industry: a review. *Int. J. Food Sci. Nutr.* **1999**, *50*, 213–224.
- (5) Caruso, F.; Caruso, R. A.; Möhwald, H. Nanoengineering of inorganic and hybrid hollow spheres by colloidal templating. *Science* **1998**, *282*, 1111–1114.
- (6) Sukhorukov, G. B.; Möhwald, H. Multifunctional cargo systems for biotechnology. *Trends Biotechnol.* **2007**, *25*, 93–98.
- (7) Schlenoff, J. B.; Decher, G. *Multilayer Thin Films: Sequential Assembly of Nanocomposite Materials*; Wiley-VCH: Weinheim, Germany, 2003.
- (8) Sukhishvili, S. A. Responsive Polymer Films and Capsules Via Layer-by-Layer Assembly. *Curr. Opin. Colloid Interface Sci.* **2005**, *10*, 37–44.
- (9) Kozlovskaya, V.; Kharlampieva, E.; Chang, S.; Muhlbauer, R.; Tsukruk, V. V. pH-Responsive Layered Hydrogel Microcapsules as Gold Nanoreactors. *Chem. Mater.* **2009**, *21*, 2158–2167.
- (10) Kozlovskaya, V.; Kharlampieva, E.; Khanal, B. P.; Manna, P.; Zubarev, E. R.; Tsukruk, V. V. Ultrathin Layer-by-layer Hydrogels with Incorporated Gold Nanorods as pH-Sensitive Optical Materials. *Chem. Mater.* **2008**, *20*, 7474–7485.
- (11) Becker, A. L.; Zelikin, A. N.; Johnston, A. P. R.; Caruso, F. Tuning the Formation and Degradation of Layer-by-Layer Assembled Polymer Hydrogel Microcapsules. *Langmuir* **2009**, *25*, 14079–14085.
- (12) Ariga, K.; Ji, Q.; Hill, J. P. Enzyme-Encapsulated Layer-by-Layer Assemblies: Current Status and Challenges Toward Ultimate Nano-devices. *Adv. Polym. Sci.* **2010**, *229*, 51–87.
- (13) Ariga, K.; Ji, Q.; Hill, J. P.; Bando, Y.; Aono, M. Forming nanomaterials as layered functional structures toward materials nanoarchitectonics. *NPG Asia Mater.* **2012**, *4*, e17.
- (14) Jang, J.; Ha, H. Fabrication of hollow polystyrene nanospheres in microemulsion polymerization using triblock copolymers. *Langmuir* **2002**, *18*, 5613–5618.
- (15) Estroff, L. A.; Hamilton, A. D. Water gelation by small organic molecules. *Chem. Rev.* **2004**, *104*, 1201–1217.
- (16) Cohen, I.; Li, H.; Hougland, J. L.; Mrksich, M.; Nagel, S. R. Using selective withdrawal to coat microparticles. *Science* **2001**, *292*, 265–267.
- (17) Discher, B. M.; Won, Y. Y.; Ege, D. S.; Lee, J. C. M.; Bates, F. S.; Dishcher, D. E.; Hammer, D. A. Polymersomes: Tough vesicles made from diblock copolymers. *Science* **1999**, *284*, 1143–1146.
- (18) Huang, H. Y.; Remsen, E. E.; Kowalewski, T.; Wooley, K. L. Nanocages derived from shell cross-linked micelle templates. *J. Am. Chem. Soc.* **1999**, *121*, 3805–3806.
- (19) Fery, A.; Weinkamer, R. Mechanical Properties of Micro- and Nanocapsules: Single-Capsule Measurements. *Polymer* **2007**, *48*, 7221–7235.
- (20) Fernandes, P. A. L.; Delcea, M.; Skirtach, A. G.; Möhwald, H.; Fery, A. Quantification of release from microcapsules upon mechanical deformation with AFM. *Soft Matter* **2010**, *6*, 1879–1883.
- (21) Tiourina, O. P.; Radtchenko, I.; Sukhorukov, G. B.; Mohwald, H. Artificial Cell Based on Lipid Hollow Polyelectrolyte Microcapsules: Channel Reconstruction and Membrane Potential Measurement. *J. Membr. Biol.* **2002**, *190*, 9–16.
- (22) Wilson, J. T.; Cui, W.; Kozlovskaya, V.; Kharlampieva, E.; Pan, D.; Qu, Z.; Krishnamurthy, V. R.; Mets, J.; Kumar, V.; Wen, J.; Song, Y.; Tsukruk, V. V.; Chaikof, E. L. Cell Surface Engineering with Polyelectrolyte Multilayer Thin Films. *J. Am. Chem. Soc.* **2011**, *133*, 7054–7064.
- (23) Carter, J. L.; Drachuk, I.; Harbaugh, S.; Kelley-Loughnane, N.; Stone, M.; Tsukruk, V. V. Truly Nonionic Polymer Shells for the Encapsulation of Living Cells. *Macromol. Biosci.* **2011**, *11*, 1244–1253.
- (24) Franz, B.; Balkundi, F.; Dahl, C.; Lvov, Y.; Prange, A. Layer-by-Layer Nano-Encapsulation of Microbes: Controlled Cell Surface Modification and Investigation of Substrate Uptake in Bacteria. *Macromol. Biosci.* **2010**, *10*, 164–172.
- (25) Balkundi, S. S.; Veerabadran, N. G.; Eby, D. M.; Johnson, G. R.; Lvov, Y. M. Encapsulation of Bacterial Spores in Nanoorganized Polyelectrolyte Shells. *Langmuir* **2009**, *25*, 14011–14016.
- (26) Donath, E.; Sukhorukov, G. B.; Caruso, F.; Davis, S. A.; Möhwald, H. Novel hollow polymer shells by colloid-templated assembly of polyelectrolytes. *Angew. Chem, Int. Ed.* **1998**, *37*, 2002–2005.
- (27) Delcea, M.; Möhwald, H.; Skirtach, A. Stimuli-Responsive LbL Capsules and Nanoshells for Drug Delivery. *Adv. Drug Delivery Rev.* **2011**, *63*, 730–747.
- (28) Skirtach, A. G.; Yashchenok, A. M.; Mohwald, H. Encapsulation, Release and Applications of LbL Polyelectrolyte Multilayer Capsules. *Chem. Commun.* **2011**, *47*, 12736–12746.
- (29) Park, M. K.; Onishi, K.; Locklin, J.; Caruso, F.; Advincula, R. C. Self-assembly and characterization of polyaniline and sulfonated polystyrene multilayer-coated colloidal particles and hollow shells. *Langmuir* **2003**, *19*, 8550–8554.
- (30) Kozlovskaya, V.; Ok, S.; Sousa, A.; Libera, M.; Sukhishvili, S. A. Hydrogen-bonded polymer capsules formed by layer-by-layer self-assembly. *Macromolecules* **2003**, *36*, 8590–8592.
- (31) Ochs, C. J.; Such, G. K.; Städler, B.; Caruso, F. Low-Fouling, Biofunctionalized, and Biodegradable Click Capsules. *Biomacromolecules* **2008**, *9*, 3389–3396.
- (32) Wang, Z. P.; Feng, Z. Q.; Gao, C. Y. Stepwise assembly of the same polyelectrolytes using host-guest interaction to obtain microcapsules with multiresponsive properties. *Chem. Mater.* **2008**, *20*, 4194–4199.
- (33) Shchepelina, O.; Kozlovskaya, V.; Kharlampieva, E.; Mao, W.; Alexeev, A.; Tsukruk, V. V. Anisotropic Micro- and Nano-Capsules. *Macromol. Rapid Commun.* **2010**, *31*, 2041–2046.

- (34) Cohen Stuart, M. A.; Huck, W. T. S.; Genzer, J.; Müller, M.; Ober, C.; Stamm, M.; Sukhorukov, G. B.; Szleifer, I.; Tsukruk, V. V.; Urban, M.; Winnik, F.; Zauscher, S.; Luzinov, I.; Minko, S. Emerging applications of stimuli-responsive polymer materials. *Nat. Mater.* **2010**, *9*, 101–113.
- (35) Angelatos, A. S.; Radt, B.; Caruso, F. Light-responsive polyelectrolyte/gold nanoparticle microcapsules. *J. Phys. Chem. B* **2005**, *109*, 3071–3076.
- (36) Biesheuvel, P. M.; Mauser, T.; Sukhorukov, G. B.; Möhwald, H. Micromechanical theory for pH-dependent polyelectrolyte multilayer capsule swelling. *Macromolecules* **2006**, *39*, 8480–8486.
- (37) Köhler, K.; Möhwald, H.; Sukhorukov, G. B. Thermal behavior of polyelectrolyte multilayer microcapsules: 2. Insight into molecular mechanisms for the PDADMAC/PSS system. *J. Phys. Chem. B* **2006**, *110*, 24002–24010.
- (38) Kinnane, C. R.; Such, G. K.; Caruso, F. Tuning the Properties of Layer-by-Layer Assembled Poly(acrylic acid) Click Films and Capsules. *Macromolecules* **2011**, *44*, 1194–1202.
- (39) Elsner, N.; Kozlovskaya, V.; Sukhishvili, S. A.; Fery, A. pH-Triggered softening of crosslinked hydrogen-bonded capsules. *Soft Matter* **2006**, *2*, 966–972.
- (40) Zhu, Z.; Sukhishvili, S. A. Layer-by-layer films of stimuli-responsive block copolymer micelles. *J. Mater. Chem.* **2012**, *22*, 7667–7671.
- (41) Ariga, K.; Mori, T.; Hill, J. P. Mechanical Control of Nanomaterials and Nanosystems. *Adv. Mater.* **2012**, *24*, 158–176.
- (42) Wilson, J. T.; Cui, W.; Chaikof, E. L. Layer-by-layer assembly of a conformal anothin PEG coating for intraportal islet transplantation. *Nano Lett.* **2008**, *8*, 1940–1948.
- (43) Sofia, S.; McCarthy, M. B.; Gronowicz, G.; Kaplan, D. L. Functionalized silk-based biomaterials for bone formation. *J. Biomed. Mater. Res.* **2001**, *54*, 139–148.
- (44) Jin, H.-L.; Kaplan, D. L. Mechanism of silk processing in insects and spiders. *Nature* **2003**, *424*, 1057–1061.
- (45) Shulha, H.; Foo, C. W.; Kaplan, D. L.; Tsukruk, V. V. Unfolding the multi-length scale domain structure of silk fibroin protein. *Polymer* **2006**, *47*, 5821–5830.
- (46) Omenetto, F. G.; Kaplan, D. L. A new route for silk. *Nat. Photonics* **2008**, *2*, 641–643.
- (47) Kharlampieva, E.; Zimnitsky, D.; Gupta, M.; Bergman, K. N.; Kaplan, D. L.; Naik, R. R.; Tsukruk, V. V. Redox-Active Ultrathin Template of Silk Fibroin: Effect of Secondary Structure on Gold Nanoparticle Reduction. *Chem. Mater.* **2009**, *21*, 2696–2704.
- (48) Shchepelina, O.; Drachuk, I.; Gupta, M. K.; Lin, J.; Tsukruk, V. V. Silk-on-Silk Layer-by-Layer Microcapsules. *Adv. Mater.* **2011**, *23*, 4655–4660.
- (49) Walletaa, B.; Kharlampieva, E.; K. Campbell-Proszowska, Kozlovskaya, V.; Malak, S.; Ankner, J. F.; Kaplan, D. L.; Tsukruk, V. V.; , Silk Layering as Studied with Neutron Reflectivity, *Langmuir*, **2012**, la300916e.
- (50) Serban, M. A.; Kaplan, D. L. pH-Sensitive Ionomeric Particles Obtained via Chemical Conjugation of Silk with Poly(amino acid)s. *Biomacromolecules* **2010**, *11*, 3406–3412.
- (51) Ye, C.; Shchepelina, O.; Calabrese, R.; Drachuk, I.; Kaplan, D. L.; Tsukruk, V. V. Robust and Responsive Silk Ionomer Microcapsules. *Biomacromolecules* **2011**, *12*, 4319–4325.
- (52) Murphy, A. R.; St John, P.; Kaplan, D. L. Modification of silk fibroin using diazonium coupling chemistry and the effects on hMSC proliferation and differentiation. *Biomaterials* **2008**, *29*, 2829–2838.
- (53) Kozlovskaya, V.; Kharlampieva, E.; Jones, K.; Lin, Z.; Tsukruk, V. V. pH-Controlled Assembly and Properties of LbL Membranes from Branched Conjugated Poly(alkoxythiophene sulfonate) and Various Polycations. *Langmuir* **2010**, *26*, 7138–7147.
- (54) Kozlovskaya, V.; Kharlampieva, E.; Mansfield, M. L.; Sukhishvili, V. Poly(methacrylic acid) hydrogel films and capsules: Response to pH and ionic strength, and encapsulation of macromolecules. *Chem. Mater.* **2006**, *18*, 328–336.
- (55) Wang, Y. J.; Caruso, F. Enzyme encapsulation in nanoporous silica spheres. *Chem. Commun.* **2004**, *13*, 1528–1529.
- (56) Shimizu, K.; Cha, J.; Stucky, G. D.; Morse, D. E. Silicatein alpha: Cathepsin L-like protein in sponge biosilica. *Proc. Natl. Acad. Sci. U.S.A.* **1998**, *95*, 6234–6238.
- (57) Tsukruk, V. V.; Singamaneni, S. *Scanning Probe Microscopy of Soft Matter: fundamentals and practices*; Wiley-VCH: Weinheim, Germany, 2012.
- (58) Elsner, N.; Dubreui, F.; Fery, A. Tuning of microcapsule adhesion by varying the capsule-wall thickness. *Phys. Rev. E* **2004**, *69*, 031802/1–031802/6.
- (59) McConney, M. E.; Singamaneni, S.; Tsukruk, V. V. Probing Soft Matter with the Atomic Force Microscopies: Imaging and Force Spectroscopy. *Polym. Polym. Rev.* **2010**, *50*, 235–286.
- (60) Chizhik, S. A.; Huang, Z.; Gorbunov, V. V.; Myshkin, N. K.; Tsukruk, V. V. Micromechanical properties of elastic polymeric materials as probed by scanning force microscopy. *Langmuir* **1998**, *14*, 2606–2609.
- (61) Kovalev, A.; Shulha, H.; Lemieux, M.; Myshkin, N.; Tsukruk, V. V. Nanomechanical probing of layered nanoscale polymer films with atomic force microscopy. *J. Mater. Res.* **2004**, *19*, 716–728.
- (62) Ibarz, G.; Däjme, L.; Donath, E.; Mohwald, H. Controlled permeability of polyelectrolyte capsules via defined annealing. *Chem. Mater.* **2002**, *14*, 4059–4062.
- (63) Glinel, K.; Dubois, M.; Verbavatz, J.-M.; Sukhorukov, G. B.; Zemb, T. Determination of pore size of catanionic icosahedral aggregates. *Langmuir* **2004**, *20*, 8546–8551.
- (64) Vinogradova, O. I. Mechanical properties of polyelectrolyte multilayer microcapsules. *J. Phys: Condens. Matter.* **2004**, *16*, R1105–R1134.
- (65) Kozlovskaya, V.; Kharlampieva, E.; Drachuk, I.; Cheng, D.; Tsukruk, V. V. Responsive microcapsule reactors based on hydrogen-bonded tannic acid layer-by-layer assemblies. *Soft Matter* **2010**, *6*, 3596–3608.
- (66) Gupta, M. K.; Singamaneni, S.; McConney, V.; Drummy, L. F.; Naik, R. R.; Tsukruk, V. V. A Facile Fabrication Strategy for Patterning Protein Chain Conformation in Silk Materials. *Adv. Mater.* **2010**, *22*, 115–119.
- (67) Lisunova, M. O.; Drachuk, I.; Shchepelina, O. A.; Anderson, K. D.; Tsukruk, V. V. Direct Probing of Micromechanical Properties of Hydrogen-Bonded Layer-by-Layer Microcapsule Shells with Different Chemical Compositions. *Langmuir* **2011**, *27*, 11157–11165.
- (68) Drachuk, I.; Shchepelina, O.; Lisunova, M. O.; Harbaugh, S.; Kelley-Loughnane, N.; Stone, M.; Tsukruk, V. V. pH-Responsive Layer-by-Layer Nanoshells for Direct Regulation of Cell Activity. *ACS Nano* **2012**, DOI: 10.1021/nn300183d.
- (69) LeMieux, M. C.; Lin, Y. -H.; Cuong, P. D.; Ahn, H. -S.; Zubarev, E. R.; Tsukruk, V. V. Microtribological and nanomechanical properties of switchable Y-shaped amphiphilic polymer brushes. *Adv. Funct. Mater.* **2005**, *15*, 1529–1540.
- (70) Jiang, C.; Wang, X.; Gunawidjaja, R.; Lin, Y. H.; Gupta, M. K.; Kaplan, D. L.; Naik, R. R.; Tsukruk, V. V. Mechanical properties of robust ultrathin silk fibroin films. *Adv. Funct. Mater.* **2007**, *17*, 2229–2237.
- (71) Kharlampieva, E.; Kozlovskaya, V.; Wallet, B.; Shevchenko, V. V.; Naik, R. R.; Vaia, R.; Kaplan, D. L.; Tsukruk, V. V. Co-cross-linking Silk Matrices with Silica Nanostructures for Robust Ultrathin Nanocomposites. *ACS Nano* **2010**, *4*, 7053–7063.
- (72) Yu, A.; Gentle, I. R.; Lu, G. Biocompatible polypeptide microcapsules via templating mesoporous silica spheres. *J. Colloid Interface Sci.* **2009**, *333*, 341–345.
- (73) Zhou, C.; Confalonieri, F.; Jacquet, M.; Perasso, R.; Li, Z.; Janin, J. Silk Fibroin: Structural Implications of a Remarkable Amino Acid Sequence. *Proteins: Struct., Funct., Genet.* **2011**, *44*, 119–122.
- (74) Kharlampieva, E.; Kozlovskaya, V.; Wallet, B.; Shevchenko, V. V.; Naik, R. R.; Vaia, R.; Kaplan, D. L.; Tsukruk, V. V. Co-cross-linking silk matrices with silica nanostructures for robust ultrathin nanocomposites. *ACS Nano* **2010**, *4*, 7053–7063.
- (75) Boudou, T.; Crouzier, T.; Auzély-Velty, R.; Glinel, K.; Picart, C. Internal Composition versus the Mechanical Properties of Polyelec-

trolyte Multilayer Films: The Influence of Chemical Cross-Linking. *Langmuir* **2009**, *25*, 13809–13819.

(76) Sukhorukov, G. B.; Antipov, A. A.; Voigt, A.; Donath, E.; Möhwald, E. pH-controlled macromolecule encapsulation in and release from polyelectrolyte multilayer nanocapsules. *Macromol. Rapid Commun.* **2001**, *22*, 44–46.

(77) Antipov, A. A.; Sukhorukov, G. B.; Donath, E.; Möhwald, H. Sustained release properties of polyelectrolyte multilayer capsules. *J. Phys. Chem. B* **2001**, *105*, 2281–2284.

(78) Glinel, K.; Sukhorukov, G. B.; Möhwald, H.; Khrenov, V.; Tauer, K. Thermosensitive hollow capsules based on thermoresponsive polyelectrolytes. *Macromol. Chem. Phys.* **2003**, *204*, 1784–1790.

(79) Ibarz, G.; Dähne, L.; Donath, E.; Möhwald, H. Resealing of polyelectrolyte capsules after core removal. *Macromol. Rapid Commun.* **2002**, *23*, 474–478.

(80) Shchepelina, O.; Lisunova, M. O.; Drachuk, I.; Tsukruk, V. V. Morphology and Properties of Microcapsules with Different Core Releases. *Chem. Mater.* **2012**, *24*, 1245–1254.

(81) Brady, R. F. *Comprehensive desk reference of polymer characterization and analysis*; Oxford University Press: New York, 2003.

(82) Domke, J.; Radmacher, M. Measuring the elastic properties of thin polymer films with the atomic force microscope. *Langmuir* **1998**, *14*, 3320–3325.

(83) Tsukruk, V. V.; Sidorenko, A.; Gorbunov, V. V.; Chizhik, S. A. Surface nanomechanical properties of polymer nanocomposite layers. *Langmuir* **2001**, *17*, 6715–6719.

(84) Lebedeva, O. V.; Kim, B. S.; Vasilev, K.; Vinogradova, O. I. Salt softening of polyelectrolyte multilayer microcapsules. *J. Colloid Interface Sci.* **2005**, *284*, 455–462.

(85) Vinogradova, O. I.; Lebedeva, O. V.; Vasilev, K.; Gong, H.; Garcia-Turiel, J.; Kim, B. S. Multilayer DNA/poly(allylamine hydrochloride) microcapsules: Assembly and mechanical properties. *Biomacromolecules* **2005**, *6*, 1495–1502.

(86) Pharr, G. M.; Oliver, W. C.; Brotzen, F. B. On the generality of the relationship among contact stiffness, contact area, and elastic modulus during indentation. *J. Mater. Res.* **1992**, *7*, 613–617.

(87) Jiang, C.; Markutsya, S.; Pikus, Y.; Tsukruk, V. V. Freely Suspended Nanocomposite Membranes as Highly-Sensitive Sensors. *Nat. Mater.* **2004**, *3*, 721–728.

(88) Markutsya, S.; Jiang, C.; Pikus, Y.; Tsukruk, V. V. Free-standing multilayered nanomembranes: testing micromechanical properties. *Adv. Funct. Mater.* **2005**, *15*, 771–780.

(89) Lavallo, P.; Voegel, J. C.; Vautier, D.; Senger, B.; Schaaf, P.; Ball, V. Dynamic Aspects of Films Prepared by a Sequential Deposition of Species: Perspectives for Smart and Responsive Materials. *Adv. Mater.* **2011**, *23*, 1191–1221.

(90) Hariri, H. H.; Schlenoff, J. B. Saloplastic Macroporous Polyelectrolyte Complexes: Cartilage Mimics. *Macromolecules* **2010**, *43*, 8656–8663.

(91) Stafford, C. M.; Harrison, C.; Beers, K. L.; Karim, A.; Amis, E. J.; Vanlandingham, A. R.; Kim, H. C.; Volksen, W.; Miller, R. D.; Simonyi, E. E. A buckling-based metrology for measuring the elastic moduli of polymeric thin films. *Nat. Mater.* **2004**, *3*, 545–550.